SLAC-PUB-2060
LBL-6466
December 1977

THE LEAD-GLASS WALL ADDITION TO THE SPEAR MARK I MAGNETIC DETECTOR*

J. M. Feller, A. Barbaro-Galtieri, J. M. Dorfan, R. Ely,
G. J. Feldman, A. Fong, B. Gobbi, G. Hanson, F. B. Heile,
J. A. Jaros, B. P. Kwan, P. Lecomte, A. M. Litke, D. Lüke,
R. J. Madaras, J. F. Martin, T. S. Mast, D. H. Miller, B. Pardoe,
S. I. Parker, M. L. Perl, I. Peruzzi, M. Piccolo, T. P. Pun,
P. A. Rapidis, M. T. Ronan, R. R. Ross, B. Sadoulet,
D. L. Scharre, T. G. Trippe, V. Vuillemin,† D. E. Yount
Lawrence Berkeley Laboratory
Northwestern University
Stanford Linear Accelerator Center
Stanford University
University of Hawaii

Abstract

A "Lead-Glass Wall," consisting of 318 lead-glass Cherenkov shower counters and three wire spark chambers, has been added to one octant of the SPEAR Mark I Magnetic Detector. The wall covers a solid angle of approximately 6% of 4π steradians and has been used to identify and measure the energies of electrons and photons produced in electron-positron collisions.

The design, calibration, gain-monitoring, and performance of the system are described.

Introduction

The Mark I Magnetic Detector is a general-purpose spectrometer for studying high-energy electron-positron collisions at the SPEAR storage ring at the Stanford Linear Accelerator Center.[1] An aluminum solenoid, 1.5 meters in radius, provides a 4 kG magnetic field. Inside the solenoid are cylindrical multiwire proportional chambers and spark chambers which measure the momenta and trajectories of charged particles. Outside the solenoid are lead-scintillator sandwich shower counters for electron and photon identification and, following the iron flux return, spark chambers for muon identification.

In the fall of 1976, one octant of the shower counters and the flux return were removed and a calorimeter consisting of 318 lead-glass Cherenkov counters and three wire spark chambers was added to the detector. This calorimeter, known as the Lead-Glass Wall (LGW), covers a solid angle of 0.69 sr, or about ten percent of the solid angle of the Mark I. The Mark I detector and the Lead Glass Wall are shown in Figure 1.

The LGW provides improved identification and energy measurement for electrons and photons. When a high-energy electron or photon enters the lead-glass it creates an electromagnetic shower. Relativistic electrons in the shower emit Cherenkov light. The total amount of light emitted is proportional to the total path length of electrons in the shower, which is in turn proportional to the amount of energy deposited in the lead-glass. The intensity of the light is measured with photomultiplier tubes attached to the lead-glass.

The Lead-Glass Wall was used to collect data from October 1976 through June 1977. During that time we gained valuable experience with the operation of a lead-glass calorimeter in an electron-positron colliding beam environment. In this paper we describe the calorimeter and its performance, with emphasis on those areas in which we encountered much more or much less difficulty than expected.

The Calorimeter

The cross section of the magnetic detector and the Lead-Glass Wall is shown in Figure 2. The lead-glass counters are in two layers, the active converters and the back blocks. The 52 active converters are each 90 cm tall, 10.8 cm wide, and 10 cm thick (3.3 radiation lengths). They are arranged in two horizontal rows of 26 counters each. Each active converter is viewed by an EMI 9531R 3.5 in. photomultiplier tube. The tubes are mounted vertically above the top row and below the bottom row.

The 266 back blocks are each 15 cm by 15 cm in cross section and 32.2 cm thick (10.5 radiation lengths). They are arranged in a matrix of 14 horizontal rows and 19 vertical columns. Each back block is viewed by an EMI 9618R 5 in. photomultiplier tube mounted horizontally on the back of the block.

There are two wire spark chambers in front of the active converters and a third chamber between the active converters and the back blocks. The entire system is enclosed in an air-conditioned box with the temperature maintained at (20±1)°C.

Because the counters were in a magnetic field (approximately 25 gauss for the back blocks and up to 150 gauss for the active converters), it was necessary to have magnetic shields which extended beyond the tube faces. To facilitate this, lucite light pipes were used between the phototubes and the lead-glass blocks. Because UVT lucite was not avaiable commercially in the right diameters, we made our own light pipes by cutting circles from 2 in.-thick lucite sheets and glueing them together in pairs to make 4 in.-long light pipes. The phototubes were joined to the light pipes with a 1/32 in. layer of General Electric RTV 615.

We had some difficulty in attaching the lucite to the lead glass. We found that the glues commonly used to attach phototubes to glass failed under temperature cycling tests because of the differing thermal expansion properties of the lucite and the lead-glass. For the active converters, we used a 1/16 in. layer of RTV 615 to join the light pipes to the lead glass. For the back blocks we desired easy removability of the phototubes and light pipes, in case replacement was required during our running. We settled on an interface of optical grease surrounded by an O-ring of Dow Corning RTV 732 to connect the light pipes to the back blocks. Because the light pipes were fairly heavy, about 14 lbs, a series of springs was employed to press the phototube and light pipe assembly against

*Work supported by the Department of Energy.

(Presented at the IEEE 1977 Nuclear Science Symposium, San Francisco, CA., October 19 - 21, 1977.)

the glass and thereby maintain about 24 lbs of pressure on the grease joint. Soon after the assembly of the LGW we discovered that large air bubbles were developing in the grease joints of some of the back blocks as the weight of the light pipes pulled them away from the glass. In response, we increased the tension in the springs so that a total of about 40 lbs of pressure was exerted. This solved the problem and slowly squeezed the air bubbles out.

As it turned out, we did not experience any phototube failures, so we never had to utilize the easy removability of the phototubes and light pipes. In fact, during the entire nine months of running, the only problems that required access to the calorimeter were occasional loose tube bases.

Signal Processing

The dynode signals from the phototubes are added together in horizontal rows. The signal from each row is fed into two latched discriminators with different thresholds for use in triggering the detector. There are three different triggers. The first requires two charged particles in the magnetic detector and is independent of the LGW. The second requires one charged particle in the magnetic detector and a minimum of about 70 MeV of energy deposited in the active converters or 150 MeV in the back blocks. The third trigger is a neutral-only trigger requiring 100 MeV of energy in the active converters plus 1 GeV in the back blocks.

The anode signals, which have a full width of about 50 ns and peak currents of the order of 1 mA, are integrated and digitized by a 328-channel Large Scale Digitizer (LSD) developed and built at the Lawrence Berkeley Laboratory.[2] The LSD provides ten-bit accuracy, which we required for sufficient dynamic range, and was designed to reduce cost and complexity by sharing common timing and control signals among a large number of ADC channels.

Gain Monitoring

In order to maintain good energy resolution and accuracy, it is necessary to monitor the gains of each of the counters as a function of time by measuring its response to a light source of known intensity. We used a single high-intensity light-emitting diode (LED), a Monsanto MV5352, as a light source. The LED illuminates a bundle of low-attenuation plastic optical fiber cables (Dupont PFX-0715) which take the light to the 318 counters. This system[3] provides each counter with a light pulse about 100 ns wide with an integrated intensity equal to that from deposition of about 2 GeV in an electron or photon shower. The exact intensity varies from counter to counter.

In order to monitor fluctuations of the intensity of the LED itself, there are three reference scintillation counters which compare the light from the LED with light from sources consisting of Americium-241 diffused in sodium-iodide crystals. Figure 3 is a schematic diagram of the gain-monitoring system. The gains were monitored once every eight hours.

We found the LED to be a more reliable light source than we expected and the Americium-NaI sources to be less reliable than expected. We had recurring problems with yellowing of the NaI due to moisture contamination when the seals of the crystal holders failed. The intensity of the LED as compared to sources that did not turn yellow did not vary by more than about two percent over the nine months of our experiment, and the LED never had to be replaced.

Although cross-checks were made with other methods, we relied on the LED monitoring system to correct all gain variations with time, including the effects of replacing ADC's and changing tube voltages as well as random fluctuations in counter gain. We estimate that we were able to monitor the counter gains to an accuracy of one to two percent. A good indication of the effectiveness of the system is that the energy accuracy and resolution of the calorimeter were not measurably degraded during the nine-month life of the experiment. This is discussed below.

Energy Calibration

The LED monitoring system corrects for all fluctuations of gain with time. It is still necessary, however, to determine an absolute calibration constant for each counter. The calibration constant relates the observed integrated pulse height to the amount of energy deposited in that counter by an electromagnetic shower. These calibration constants are determined by using electron-positron elastic scattering events (Bhabha scattering). These events provide electrons whose energy is equal to the beam energy and is thus well known. Such events are easily identified, and the momentum measurement in the magnetic detector is used to remove events in which a significant amount of energy is lost by radiation from the interaction vertex.

We used about 5000 Bhabha scattering events from the first three months of running (October-December 1976) for the calibration. Each event provides an equation of the form

$$\sum_i C_i A_i = E_{beam}$$

where the C's are the 318 unknown calibration constants, the A's are the integrated pulse heights from the lead-glass counters after correction for gain variations with time as measured by the LED monitoring system, and E_{beam} is the colliding beam energy. For this sample, E_{beam} varied between 3.2 and 3.7 GeV. The sum is taken only over those active converters and back blocks which are near the projected electron track as determined by the spark chambers of the magnetic detector. We find the calibration constants by a least squares solution to this system of 5000 equations in 318 unknowns.

Energy and Position Resolution

The energy resolution of the Lead-Glass Wall is limited by the presence of the aluminum magnet coil, which is 1 radiation length thick, in front of the LGW. Energy losses in the coil degrade the resolution. In preliminary tests with a subset of the LGW in an electron beam, we found that the energy resolution of the calorimeter for electrons could be approximately described by the function $\sigma/E = 5\%/\sqrt{E}$, E in GeV, without the presence of the aluminum and $\sigma/E = 9\%/\sqrt{E}$ with 1 radiation length of aluminum in front of the lead-glass. Subsequently, we found we were able to reproduce this resolution with the entire LGW under actual running conditions over a period of nine months.

Figure 4 shows the distribution of the measured energy in the LGW divided by the colliding beam energy for the electrons from Bhabha scattering used in the calibration. The average electron energy is 3.5 GeV. The resolution is about 4.8%.

Figure 5 shows the same distribution for 1.89 GeV electrons in data taken in May and June 1977. The distribution is broader than in Figure 4 because the electron energy is lower. The peak is centered at 1.0 and the resolution is about 6.7%, in agreement with the $9\%/\sqrt{E}$ expected from our test beam results. The data in Figure 5 were taken over a period of two months and were taken six months after the calibration of the LGW. The fact that the energy resolution and accuracy are not measurably degraded demonstrates the stability of the system and the effectiveness of the LED monitoring system in tracking the counter gains. The resolution as a function of energy is shown in Figure 6.

Events of the type $e^+e^- \to \gamma\gamma$ provide photons of known energy and thereby allow us to check the energy resolution for photons. Figure 7 shows the measured energy divided by the beam energy for 1.89 GeV photons. There is a lot of background because these events are harder to identify cleanly in the magnetic detector than are the Bhabha scattering events. We have used the spark chambers in front of the active converters to detect electrons from photons which converted in the magnet coil. For those photons we have added 40 MeV to the measured energy in order to compensate for energy lost in the coil. In this way we get an energy resolution which is slightly better than that for electrons. The resolutoin in this plot is 5.8%. Our energy resolution for photons can be approximately described by $\sigma/E = 8\%/\sqrt{E}$.

We measure the position of a shower in the active converters and in the back blocks by taking the centroid of the distribution of energy deposited. This provides two-dimensional information from the back blocks, but the active converters contribute useful information only in the horizontal coordinate since they are 90 cm tall. We determine the position resolution by comparing the position determined in this manner with the projected track position for electrons from Bhabha scattering. The distribution of this difference in the horizontal coordinate in the back blocks for electrons from 3.2 to 3.7 GeV is shown in Figure 8. Sigma for this plot is about 3 cm. We find that this resolution does not vary significantly over the energy range 1.5-3.7 GeV.

The spark chambers of the LGW provide an additional measurement of the position of a shower. In the third spark chamber, which is behind a total of four radiation lengths of material, we are able to find the position of a shower with a resolution of about 2 cm in each of the two dimensions in the spark chamber plane by taking the centroid of the distribution of sparks. This resolution was determined using electrons from Bhabha scattering, as above. We expect the resolution for photons in the third spark chamber to be about the same. The position resolution for electrons in the first two spark chambers, which are behind only one radiation length of material, is about 1.5 cm, but this does not necessarily apply to photons because after only one radiation length the properties of electron and photon showers are different.

We determine the direction of photons in the LGW by combining the information from the spark chambers and the two layers of lead-glass. The average angular resolution for photons is about 0.5 degrees.

Combining the energy and angular measurement, we determine the invariant mass of pairs of photons in the LGW to reconstruct neutral pions. Figure 9 is an invariant mass distribution for two-photon combinations in which each photon has a measured energy of at least 150 MeV. The neutral pion peak is clear.

Electron Identification

In our experiment we wished to find electrons from decays of heavy leptons and charmed particles in the center-of-mass energy region from 3.7 to 7.4 GeV. This required separation of electrons from hadrons in the momentum region below 1 GeV/c. We accomplished this with cuts on the energy deposited in the active converters, in the back blocks, and in the two layers combined. In the active converters we required at least 150 MeV or 25% of the particle's momentum, whichever was greater. In the back blocks we required at least 10% of the particle's momentum, and in the wall as a whole we used a sliding cut varying from 63% of the momentum at 300 MeV/c to 80% at 1.4 GeV/c. We determined the probability for a hadron to pass these cuts by running at the $\psi(3.1)$, below the threshold for production of heavy leptons and charmed particles. We eliminated electrons from photon conversions in the beam pipe by removing from consideration pairs of oppositely charged particles with a small opening angle. Assuming that all other particles in multiprong events at the $\psi(3.1)$ were hadrons, we determined the probability for a hadron to simulate an electron to be falling with increasing momentum from 1.4% at 300 MeV/c to 0.4% at 1 GeV/c. These figures represent upper limits because there were some electrons present from hadron decays and from photon conversions where the second electron was not detected because its momentum was below the detector cutoff of about 100 MeV/c. We estimate that the latter effect accounts for about one fourth of the observed misidentification probabilities.

We determined our efficiency for correctly identifying electrons by using electrons from the processes $e^+e^- \to e^+e^-\gamma$ and $e^+e^- \to e^+e^-e^+e^-$. The efficiency rises with momentum from about 55% at 300 MeV/c to 90% at 1 GeV/c.

These efficiencies and misidentification probabilities apply only to the set of cuts described above. Depending on the momentum region of interest and the demands of a particular experiment, the cuts could be varied to provide the optimum trade-off between efficiency and background.

Summary

We have used a lead-glass calorimeter to study high-energy electron-positron collisions at SPEAR over a period of nine months. We have monitored the gains of the lead-glass counters with a single LED connected to the counters by fiber optics. The energy resolution of the system, which is limited by the presence of 1 radiation length of aluminum in front of the calorimeter, has been $9\%/\sqrt{E}$ for electrons and $8\%/\sqrt{E}$ for photons. We have identified electrons with an efficiency rising from 55% at 300 MeV/c to 90% at 1 GeV/c and a probability for a hadron to be identified as an electron falling from less than 1.4% at 300 MeV/c to less than 0.4% at 1 GeV/c.

Acknowledgements

We would like to thank N. Andersen, R. Baggs, S. Buckingham, T. Daley, G. Gibson, S. Hand, P. Harding, C. Hoard, E. Lee, R. Leonard, M. Long, C. MacDonald, L. Sheriffe, G. Smith, R. Smits, R. Stickley, and H. Van Slyke for their invaluable contributions to the design and construction of the Lead-Glass Wall.

Footnotes and References

*This work was done with support from the U. S. Energy Research and Development Administration.

†Fellow of the Swiss National Fund for Scientific Research.

1. J. E. Augustin, et al., Phys. Rev. Lett. 34, 233 (1975), F. Vannucci et al., Phys. Rev. D15, 1814 (1977).

2. R. F. Althaus, et al., IEEE Trans. Nucl. Sci. NS-24, 408 (1977).

3. R. J. Madaras, et al., "An LED Monitoring System for a Large Lead-Glass Array," Lawrence Berkeley Laboratory Report LBL-6767 (in preparation).

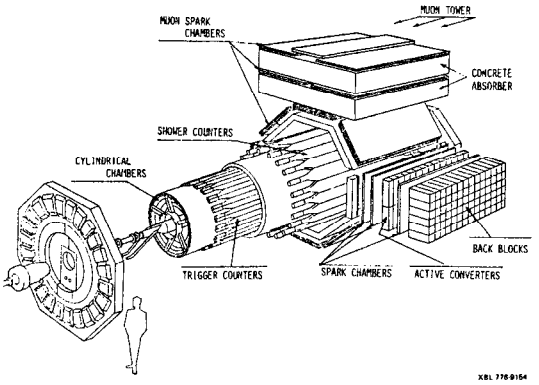

Fig. 1. Exploded view of the SPEAR Mark I Magnetic Detector with the Lead-Glass Wall. The active converters and the back blocks are the two layers of lead-glass.

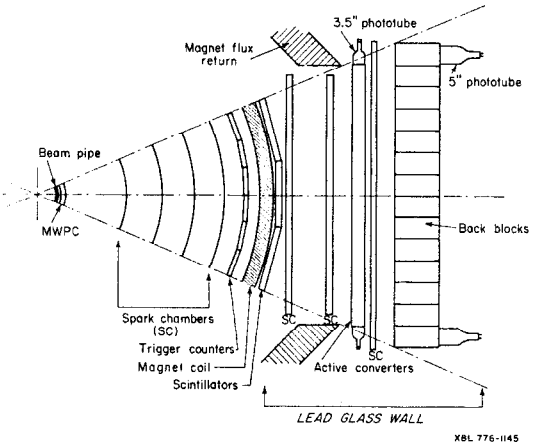

Fig. 2. Cross-section of the SPEAR Mark I Magnetic Detector with the Lead-Glass Wall.

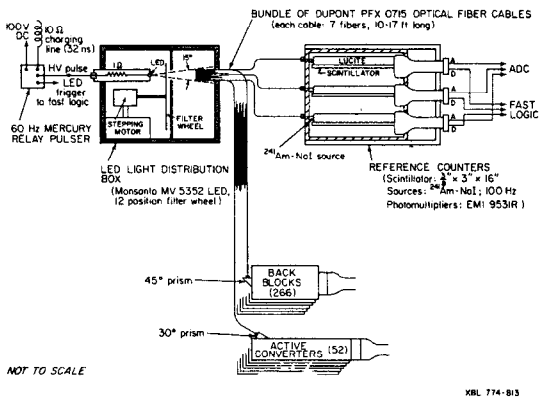

Fig. 3. Schematic diagram of the LED monitoring system for the Lead-Glass Wall.

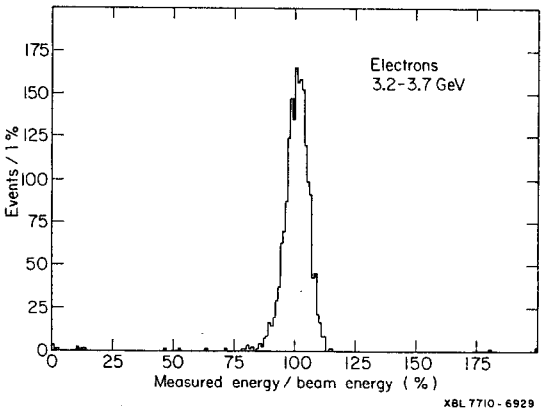

Fig. 4. Measured energy in the Lead-Glass Wall divided by the colliding beam energy for electrons from Bhabha scattering between 3.2 and 3.7 GeV. The resolution is $\sigma/E = 4.8\%$.

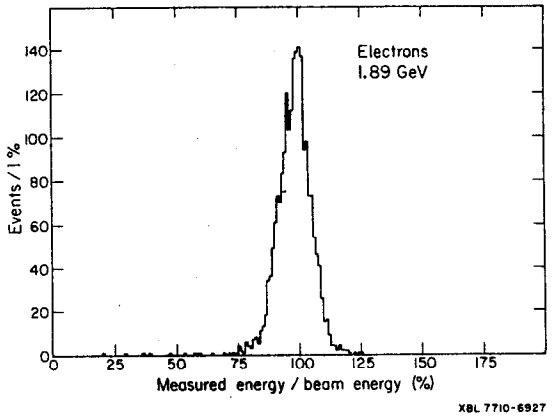

Fig. 5. Measured energy in the Lead-Glass Wall divided by the colliding beam energy for electrons from Bhabha scattering at 1.89 GeV. The resolution is $\sigma/E = 6.7\%$.

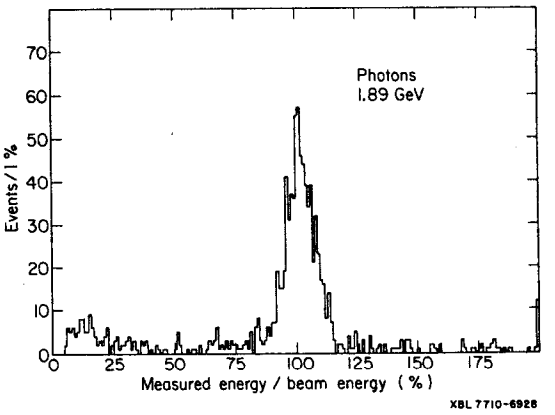

Fig. 7. Measured energy in the Lead-Glass Wall divided by the colliding beam energy for photons from the reaction $e^+e^- \to \gamma\gamma$ at 1.89 GeV. The resolution is $\sigma/E = 5.8\%$.

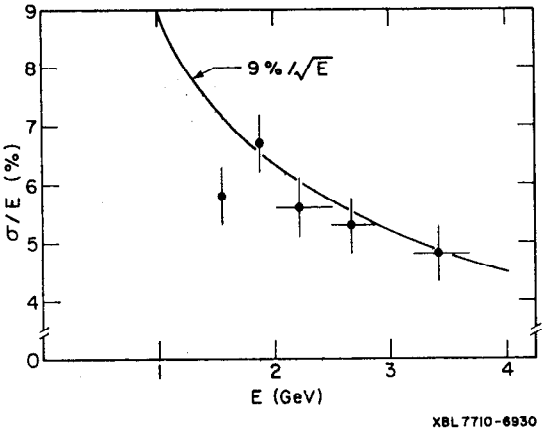

Fig. 6. Energy resolution as a function of energy for electrons in the Lead-Glass Wall, as determined from Bhabha scattering events. The curve is at $\sigma/E = 9\%/\sqrt{E}$, the resolution obtained in a test beam with a subset of the Wall. In both cases there was one radiation length of aluminum in front of the lead-glass.

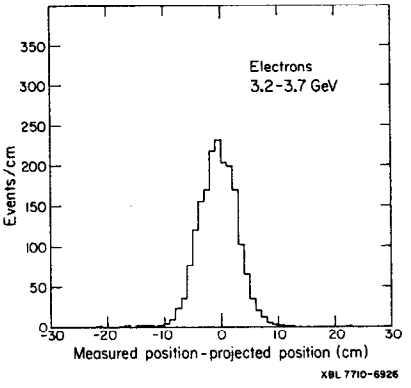

Fig. 8. Measured position in the Lead-Glass Wall minus the projected track position in the horizontal coordinate for electrons from Bhabha scattering between 3.2 and 3.7 GeV. The resolution is 3 cm.

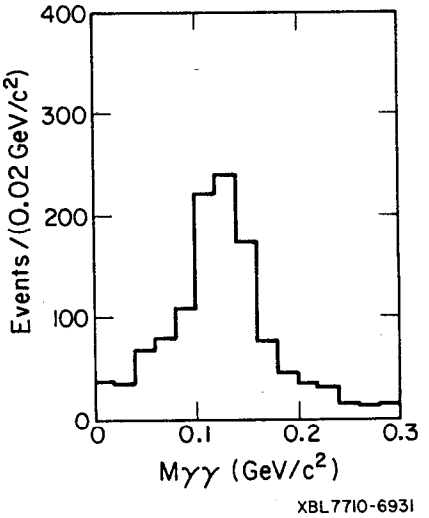

Fig. 9. Two-photon mass spectrum for pairs of photons in the Lead-Glass Wall. Only combinations with both photons having E > 150 MeV are plotted.